# DRILL STRING VIBRATION MODELING INCLUDING COUPLING EFFECTS

## H. Ahmadian,  S. Nazari  and  H. Jalali

***Abstract:*** *The governing equations of motion for a drill string considering coupling between axial, lateral and torsional vibrations are obtained using a Lagrangian approach. The result leads to a set of non-linear equations with time varying coefficients. A fully coupled model for axial, lateral, and torsional vibrations of drill strings is presented. The bit/formation interactions are assumed to be related to the following parameters: bit motion, effects of gyroscopic moments, contact with the borehole wall, axial excitation due to bit/formation interactions, and hydrodynamic damping due to the presence of drilling mud. Simulation results show that parametric resonance and whirling may occur simultaneously within the range of operating conditions of drilling. The contact force between collar and borehole wall is calculated and its behavior is investigated. The dynamic behavior is quite complicated and may become non-periodic, suggesting a chaotic behavior.*

***Keywords:*** *Drill string, Critical speed, Whirling, Parametric resonance, Coupling effects.*

## 1. Introduction

The lower part of a drill string used for the drilling of oil or gas wells is usually composed of drill collars and stabilizers as shown in figure (1). The drill string rotates during drilling, with a typical borehole diameter ranging from 100 to 850mm, while drill collars have a diameter between 100 to 200mm and a wall thickness up to 85mm. Stabilizers distances varies between 5 to 50m. During drilling operations for oil wells, severe vibrations occur that are detrimental to the service life of drill strings and down-hole equipment.

The causes of these vibrations include impact and friction at the borehole/drill string and bit/formation interfaces, imbalances, eccentricity or initial curvature in the drill collar sections, various linear or non-linear resonances.

Axial, lateral, and torsional vibrations are generally quite complex in nature. Phenomena such as bit bounce, stick-slip, forward and backward whirl and parametric instabilities have been shown to occur. It is well known that drill string vibrations may lead to fatigue failures and abrasive wear of tubulars, damaging the drill bit and the borehole wall.

As a consequence, oil well drilling becomes inefficient and costly. On the other hand, measurements of these vibrations may provide valuable information about the drilling assembly and formation characteristics. Therefore vibration must be fully understood and their

effects should be minimized by any approach to drilling optimization.

Many studies on drill string dynamics are mostly concerned with axial and tensional vibrations. The coupling between these two motions is discussed in [1]. Increasing the rotary speed may cause lateral problems such as backward and forward whirling, impacts with the borehole wall and parametric instabilities [2]. It is desirable to extend the range of safe drilling speeds and to achieve this, a proper understanding of the coupled dynamics of drill string s is necessary. Vandiver *et. al.* [3] studied the bending vibration of rotating and non-rotating drill string s and considered the whirling and parametric instabilities. However, intermittent contact with the borehole wall was not addressed.

A detailed study on whirling was carried out by Jansen [4] and Jansen *et. al.* [5] including the effects of impact with the borehole wall. Using a lumped parameter model, it was concluded that the resulting unstable drill collar motion could be periodic or chaotic. Abbassian et. al. [6] investigated the stability of drill string considering three simple mechanical systems representing string-torsional vibration, bit-lateral dynamics, and coupled torsional-lateral vibration of the bit string assembly. Christoforou et. al. [7] developed a non-linear model for a non-rotating drill string. Lateral vibrations which occur in the forms of whirling and parametric resonance have also been studied extensively [8]. In these studies, the torsional vibrations are not considered and the drill string is assumed to rotate at a constant speed. Consequently, the excitation due to bit/formation interaction was assumed to be a

***H. Ahmadian, S. Nazari & H. Jalali,*** Department of Mechanical Engineering, Iran University of Science & Technology, Tehran. ahmadian@iust.ac.ir, s.nazari@iust.ac.ir, jalali@iust.ac.ir

prescribed function of time. Yigit e. al. [9] studied the coupled torsional and lateral vibrations and the excitation at the bit was assumed to be related to the rotating of the bit. Recently Khulief and Al-Naser [10] derived a finite element formulation representing the dynamic behavior of drill string  by employing Lagrangian approach.

Their model accounts for the gyroscopic effect, the torsional/bending inertia coupling, and the effect of the gravitational force field. In another paper Khulief, Al-Sulaiman and Bashmal [11] formulated a dynamic model of the drill string including the drill-pipes and drill-collars.

The equation of motion of the rotating drill string was derived using Lagrangian approach in conjunction with the finite element method. The model accounted for the tensional–bending inertia coupling and the axial–bending geometric nonlinear coupling.

In addition, the model accounted for the gyroscopic effect, the effect of the gravitational force field, and the stick–slip interaction forces. In the present paper, coupled torsional-bending-axial motions of the drill strings in presence of bit motion, effects of gyroscopic moments, contact with the borehole wall, axial excitation due to bit/formation interactions, and hydrodynamic damping due to the presence of drilling mud are investigated.

Simulation results show that parametric resonance and whirling may occur simultaneously within the range of operating conditions of drilling. The contact force between collar and borehole wall is calculated and its behavior is investigated. The dynamic behavior is quite complicated and may become non-periodic, suggesting a chaotic behavior.

## 2. Modeling

The bottom hole assemble (BHA) is usually composed of drill collars and stabilizers as shown in figure (1). The lower portion of the drill collars supported by the stabilizer is under compression due to the weight of the upper portion of the drill collars.

The compressive force applied at the bit, termed weight-on-bit (WOB), is the essential force for the drilling. In this study, the lower portion of the drill collars is assumed to be under combined torsional, axial and lateral vibrations and the rest of the BHA is assumed to be undergoing axial vibrations. This assumption can be justified by considering that in most real applications the upper portion of the BHA is in permanent contact with the borehole wall. The transverse motion of the collars is confined by the borehole and is assumed to be adequately modeled as a Raleigh beam theory with simply supported boundary conditions at the stabilizer locations. The drill string  is assumed to be a hollow cylinder with uniform cross-section and rotate about and undergoing transverse vibration which results in gyroscopic effects (Fig2).The equations of motion are obtained using Lagrangian approach assuming known modes of vibrations.

First the axial-lateral vibrational behavior is modeled. Next the torsional vibrations are included in the model. The result is a set of non-linear coupled equations which should be solved numerically.
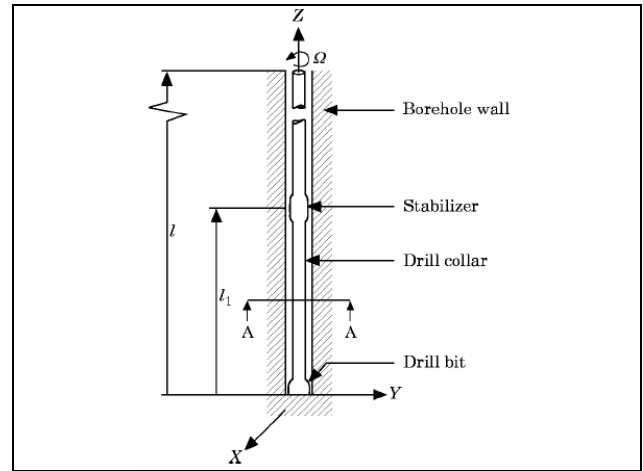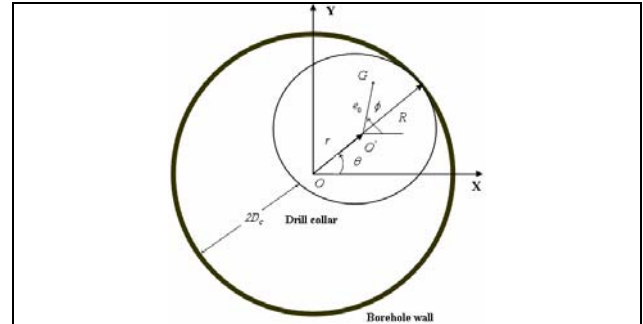

**Fig 1. A schematic of the system**


**Fig 2. Section A-A trough a borehole and deflection drill collar**

### 2.1. Model Including Axial-Lateral Vibration
In developing the axial-lateral vibrations of rotating drill string  the total kinetic energy can be written as [12]:

$$T = \frac{1}{2}\rho A \int_0^l \left( w_t^2 + u_t^2 + v_t^2 e_0^2 \Omega^2 + 2e_0\Omega(v_t\cos\theta - w_t\sin\theta) \right. $$
$$\left. \rho I\left(w_{tz}^2 + v_{tz}^2 + 2\Omega^2 - 2\Omega(w_{tz}v_z + v_{tz}w_z)\right)\right)dz \qquad (1)$$

where $d_{pq} = \dfrac{\partial^2 d}{\partial p \partial q}$, $l$ is the total BHA length, $\rho$ is the density of the material, $A$ is the cross sectional area, $I$ is the cross sectional moment of inertia and $\Omega$ is drilling angular velocity. $v$, $w$ and $u$ are respectively deformations in directions X, Y and Z (Fig. 1).  The strain energy due to axial and transverse deformations can be expressed as:

$$V = \frac{1}{2}\int_0^l \left( EA\left(u_z + \frac{1}{2}\left(v_z^2 + w_z^2\right)\right)^2 + EI\left(w_{zz}^2 + v_{zz}^2\right)\right)dz \qquad (2)$$

where E is Young's modulus. In equation (2) the non-linear axial strain produces the coupling between the axial and transverse deflections.

The virtual works due to external forces are also taken into considerations in developing the equations of motions. These forces are the contact force between borehole and the collar, the damping force result from hydrodynamic drag of drilling mud, the gyroscopic moments, and the axial force.

The contact force between borehole and the collar is defined using the Hertzian law as:

$$F_N = \begin{cases} -K_h(r-D_c)^{\left(\frac{3}{2}\right)} & if \quad |r| \geq D_c \\ 0 & if \quad |r| < D_c \end{cases} \tag{3}$$

where $K_h$ is the Hertizan stiffness, a parameter which depends on the material properties and the contact geometry [13], and $D_c$ is the borehole clearance. The virtual work due to contact force is:

$$\delta w_{cont} = \int_0^l \frac{F_N}{r} \left( (w - sign(V_{pc})\mu v)\delta w + \right. \\ \left. + (v + sign(V_{pc})\mu w)\delta v \right)\delta(z - z_c)dz \tag{4}$$

where $z_c$ is impact location. The velocity of the collar at the contact point given as:

$$V_{pc} = r_c\phi_t + R\Omega \tag{5}$$

where $r_c$ is the position of the geometric center at the impact location and $\phi$ is given by:

$$\phi = \arctan\left(\frac{v}{w}\right) \tag{6}$$

A damping force resulting from hydrodynamic drag of mud is also acting on the collar. The virtual work due to this force is considered as:

$$\delta w_{hyd} = -\rho_f C_D R \int_0^l \left( (w_t\delta v + v_t\delta w)\sqrt{w_t^2 + v_t^2} \right)dz \tag{7}$$

where $\rho_f$ is the density of the drilling mud and $C_D$ is the hydrodynamic drag coefficient. For a rotating drill string , gyroscopic moments result from the change in the angular momentum in its bending motion. The virtual work of such moment can be written as:

$$\delta w_{gy} = \int_0^l \left\{ J_P\Omega w_{xt}\delta w - J_P\Omega v_{xt}\delta v \right\}dz \tag{8}$$

where $J_P$ is the cross section mass moment of inertia. Finally, the axial WOB excitation, and bit formation interaction can be expressed as:

$$P(t) = P_0 + P_f \sin(n\Omega t) \tag{9}$$

$P_0$, $P_f$, $n$, and $\Omega$ are the static component of the WOB, the amplitude of fluctuating component, the bit constant, and the drilling angular velocity, respectively. The virtual work due to axial force is:

$$\partial w_P = \int_0^l P(t)\delta u dz \tag{10}$$

All component of potential and kinetic energy and virtual work of forces are defined. The governing equations of system can be derived by using Lagrange's equation:

$$\frac{d}{dt}\left(\frac{\partial T}{\partial q_i^\bullet}\right) - \frac{\partial T}{\partial q_i} + \frac{\partial V}{\partial q_i} = Q_i \tag{11}$$

The equations of motion for coupled axial-lateral vibrations are obtained by using assumed mode method:

$$u = u_{st} + \sum_{i=1}^M \varphi_i(z)\alpha_i(t) \tag{12}$$

$$v = \sum_{j=1}^N \zeta_j(z)\beta_j(t) \tag{13}$$

$$w = \sum_{k=1}^R \zeta_k(z)\gamma_k(t) \tag{14}$$

In equations (12)-(14) the unknowns $\alpha_i(t)$, $\beta_j(t)$ and $\gamma_k(t)$ are generalized coordinates, $\varphi_i(z)$ and $\zeta_j(z)$ are sets of admissible function that satisfy the geometric boundary conditions in axial and lateral motions, respectively. The deformation $u_{st}$ is due to the axial load given as:

$$u_{st} = \begin{cases} \dfrac{P(t)}{EA}z & 0 \leq z \leq l_1 \\ \dfrac{P(t)}{EA}l_1 & l_1 \leq z \leq l \end{cases} \tag{15}$$

The admissible functions $\varphi_i(z)$ are selected as the normalized mode shapes of a simply supported beam in axial motion,

$$\varphi_i(z) = \sqrt{\frac{2}{\rho A L}} \sin\left( (2i-1)\frac{\pi z}{2L} \right) \tag{16}$$

and $\zeta_j(z)$ are chosen as normalized mode shapes for the fixed-free bar in transverse motion:

$$\zeta_k(z) = \sqrt{\frac{2}{\rho A L}} \sin\left( \frac{k\pi z}{L} \right) \tag{17}$$

Substituting equations (15)-(17) into equation (1)-(10) and applying Lagrange's equation for general coordinate, a set of non-linear ordinary differential equations for coupled axial-lateral vibration is obtained. These equations are shown in Appendix A.

## 2.2. Inclusion of Torsional Vibration Effects

Torsional vibrations in drill string play an important role in many issues of drilling such as rate of penetration (ROP), over-torque drill pipe connection, twist-offs, premature bit wear and etc.

These vibrations can be observed either as fluctuations in the current through the electric motor that drives the rotary table. Commonly torsional vibrations in drill string are observed in three parts, namely between motor and rotary surface, drill pipe and drill collar. The drill collar is assumed to be rigid in torsional vibration since the collars are much stiffer than the drill pipe.

Torsional vibration in drill pipes and collar are very important. Due to these torsional vibrations the angular velocity of rotary surface varies with time ([1],[5]). In some studies the variation in angular velocity of the rotary table is defined using sinusoidal functions [9]. In present study, torsional vibrations of the parts between motor and rotary table and drill pipe are investigated and the torsional vibration is assumed coupled with the axial and the lateral vibrations. In figure (3) the power transmission system consisting of motor, rotary table and drill pipe is shown.
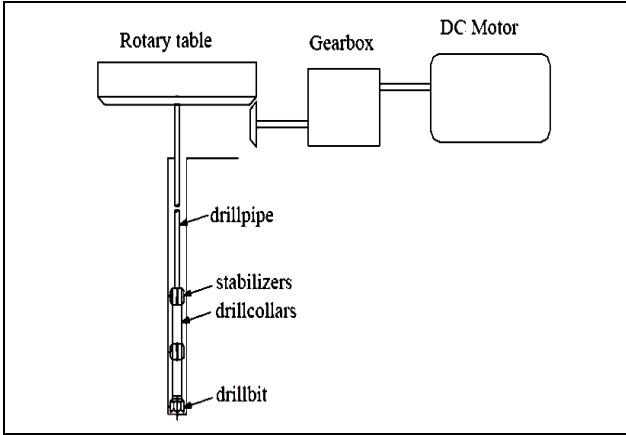


**Fig 3. Power transmission system**

The equations of motion for torsional vibration are obtained as:

$$J_T \frac{\partial^2 \phi_T}{\partial t^2} - K_{dp}(\lambda - \phi_T) = K_{up}(\Omega t - \phi_T) + C_{up}(\Omega - \frac{\partial \phi_T}{\partial t}) \qquad (18)$$

$$J_C \frac{\partial^2 \lambda}{\partial t^2} + K_{dp}(\lambda - \phi_T) = T_{Bit} + T_{cont} \qquad (19)$$

where $\Omega$, $\dot{\phi}_T$ and $\dot{\lambda}$ are, the motor, the rotary table, and the bit angular velocities, respectively. $J_T$ is mass moment of inertia of rotary table plus 2/3 of drill pipe mass moment of inertia. $K_{dp}$ is equivalent torsion stiffness of the drill pipe, $K_{up}$, and $C_{up}$ are torsion stiffness and damping of power parts , $J_C$ is mass moment of inertia for BHA which includes drill collar and 1/3 of drill pipe mass moment of inertia. $T_{Bit}$ is the torque from bit and $T_{cont}$ is the torque due to tangential force of contact between well and collar. Main parameters in bit torque are weight on bit (WOB), type of bit and bit speed. There are several models for bit interaction torque ([5], [6], [14], [9]). In this study the model offered in reference [6] is adopted, i.e.:

$$T_{Bit} = W \left( f_0 + f_t e^{-\gamma \dot{\lambda}} \right) \qquad (20)$$

where W is WOB, $f_0$, $f_t$ are bit constants, and $\gamma$ is the decay parameter. The torque due to tangential contact force is expressed as:

$$T_{cont} = -sign(V_{pc})\mu K_h(r - D_c)^{\left(\frac{3}{2}\right)} \times \\ Heaviside(r - D_c)R \qquad (21)$$

The governing equations can now be derived by combining axial-lateral vibration equations derived in section 2.1 with torsional equations (18) and (19) with the variables $\alpha_i(t), \beta_j(t), \gamma_k(t)$ and $\phi_T(t), \lambda(t)$. This yields the set of coupled ordinary non-linear differential equations shown in Appendix A.

The obtained governing equations are coupled non-linear differential equation with time varying coefficients. The axial and lateral motions are coupled due to non-linear elastic deflections and torsional and lateral motions are coupled due to contact torque and variation of angular velocity of rotary table due to torsional vibrations.

The transverse motions in the x and y directions are coupled due to gyroscopic moments, hydrodynamic damping, and impact and friction forces. The time varying coefficients are due to the axial excitations and axial-transverse coupling. The governing equations also contain harmonic excitations due to the axial force generated by the bit, and out of balance mass. in the next section the numerical solution of the obtained equations is presented and the coupling effects are investigated.

## 3. Numerical Simulations

In the numerical simulations, the axial and lateral deformations are approximated each with one mode only.

In addition, an initial static deflection due to weight force is implemented in axial deformations. Clearly, the existence of impacts would require a multi-mode analysis which will increase the dimension and complexity of the non-linear problem.

Since the objective of this work is to improve the understanding of the coupling effects of torsional, lateral and axial motions, and interactions between various phenomena such as whirling, parametric excitation, etc.

Therefore one-mode approximation for the deformations is adequate. Note that the one-mode approximation used for the transverse motion also simplifies the contact condition in that the impact always occurs at the mid-span of the last drill collar section. A numerical procedure is employed to solve the set of obtained equations. The problem is solved using Runge-Kutta method in MATLAB (command line ODE45). The parameters used in the simulation are shown in table (1), which represent a typical case in an oil well drilling operation.

Number of simulations were carried out assuming the bit factor n=1. In this case the forcing frequency, $n\Omega$ is equal to the rotating speed and the critical whirling speed is 5.725m/s. The dynamic response of collar in lateral motion at the rotating speed 4.8 rad/s for uncoupled torsion and fully coupled model is shown in Fig. 4 and 5.

**Table 1. The parameters of a typical oil well**

| $l_1$ $(m)$ | 20 | $\mu$ | 0.1 |
|---|---|---|---|
| $l$ $(m)$ | 1000 | $\gamma$ | 0.02 |
| $\rho$ $(Kg/m^3)$ | 7800 | $f_t$ | 0.0762 |
| $E$ $(GPa)$ | 210 | $K_{up}$ $(N/m)$ | 90 |
| $K_h$ $(N/m)$ | $6.71 \times 10^{11}$ | $C_{up}$ $(Ns/m)$ | 1342 |
| $D_c$ $(m)$ | 0.05 | $e_0$ $(m)$ | 0.0065 |
| $\rho_f$ $(Kg/m^3)$ | 1500 | $P_0$ $(N)$ | $-1 \times 10^5$ |
| $P_f$ $(N)$ | $-50 \times 10^3$ | | |

In this situation the full coupled model predicts the contact between collar and well but amplitude of vibration in axial-lateral model is smaller than clearance between collar and wall. Due to the presence of dissipative effects such as friction and hydrodynamic damping, the vibrations eventually settle into a limit cycle behavior.
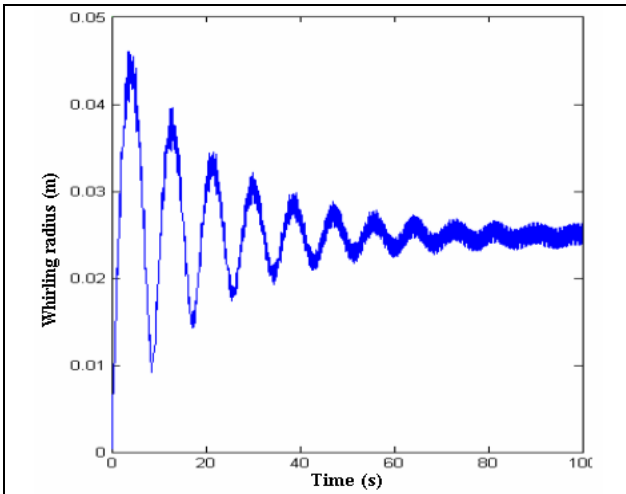


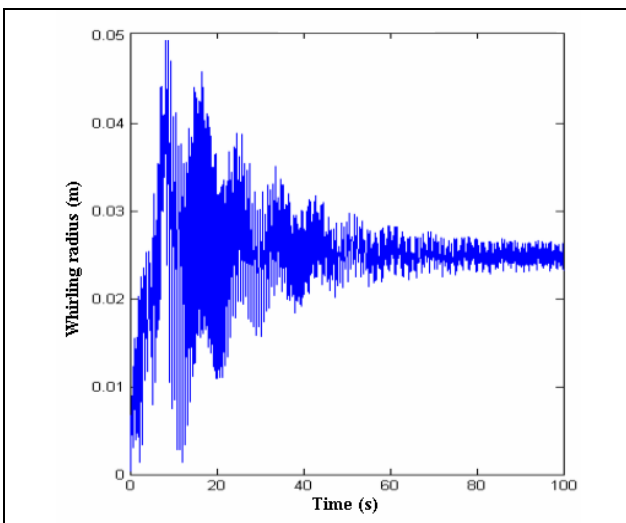**Fig 4.** Deflection at $\Omega = 4.8$ **rad/s for axial-lateral model**



**Fig 5.** Deflection at $\Omega = 4.8$ **rad/s for fully coupled model**

When the rotating speed is increased to 5.725 rad/s it is equal to the estimated critical whirling speed. The response for this case is shown in Fig. 6 and 7 and as expected the whirling amplitudes are larger than those of the previous case.
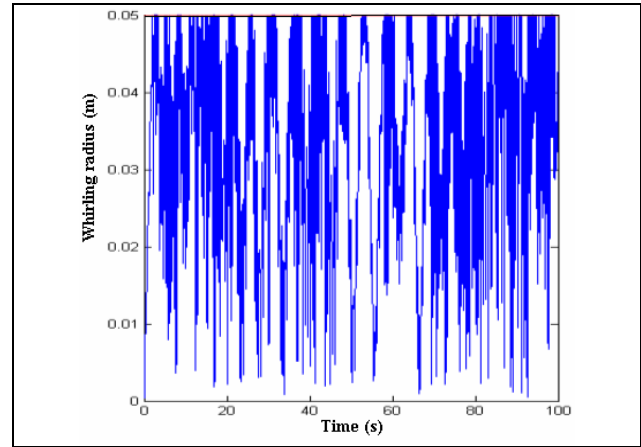


**Fig 6.** Deflection at $\Omega = 5.725$ **rad/s for axial-lateral model**

More information about the whirling behavior can be obtained by observing the whirling speed shown in Fig. 8 and 9. For the time period covered by the simulation the whirl direction continuously changes between forward and backward.
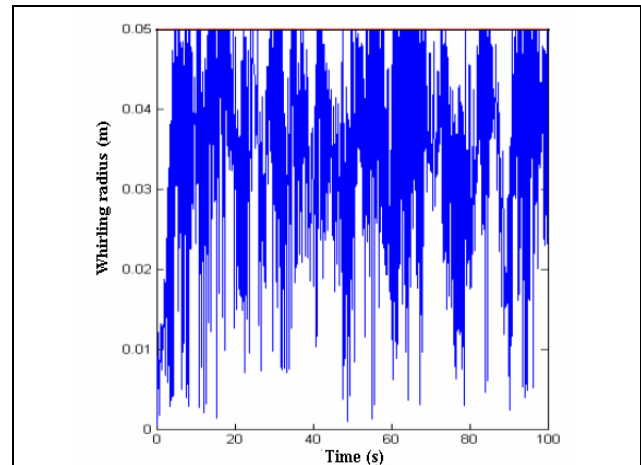


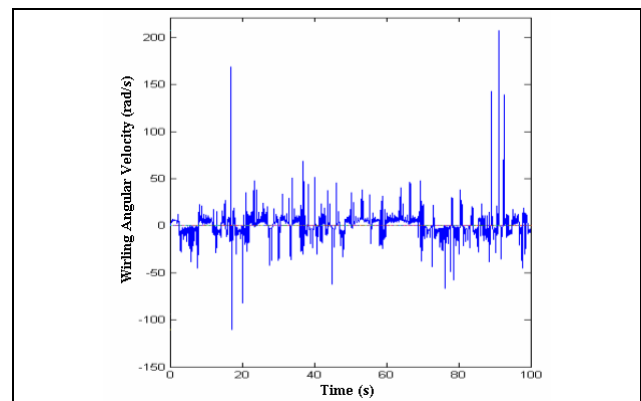**Fig 7.** Deflection at $\Omega = 5.725$ **rad/s for coupled model**



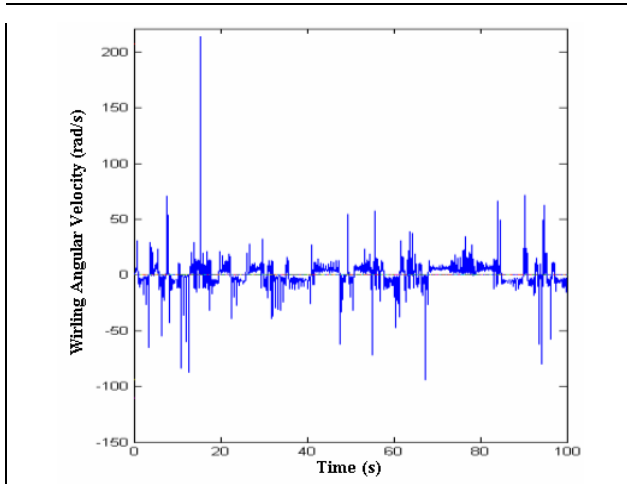**Fig 8.** Whirling speed at $\Omega = 5.725$ **rad/s for axial-lateral model**

**Fig 9. Whirling speed at $\Omega = 5.725$ rad/s for fully coupled model**

Next the angular velocity is increased to 8 rad/s, and the resulting dynamic response is shown in Fig. 10 and 11.

At this speed the axial-lateral model don't predict any contact but the fully coupled model shows contact between collar and well. The maximum angular velocity that axial-lateral model is predicting contact at this case is equal 6.8 m/s.

However when the torsional vibration is coupled with the axial-lateral model the predictions for contact starts at lower speeds and ends at higher speeds comparing to the predictions of the model with no coupling effects between torsional and other motions. Consequently the fully coupled model increases the range of critical angular velocity of drill string. The coupling between axial-lateral vibrations affects the natural frequencies in lateral motion [7]. However the coupling between torsional and to axial-lateral motions doesn't have any effect on theses frequencies. This can be seen by observing that the critical speeds in both models are the same. Both models have the same critical angular velocity but the responses of the models at the same velocities are not same.
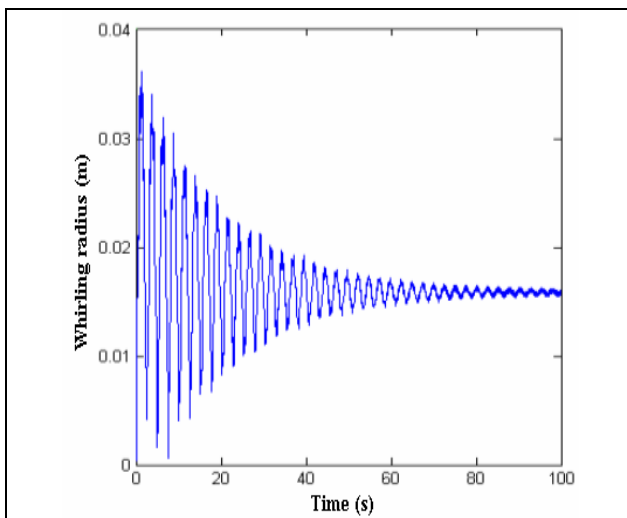


**Fig 10. Deflection at $\Omega = 8$ rad/s for axial-lateral**
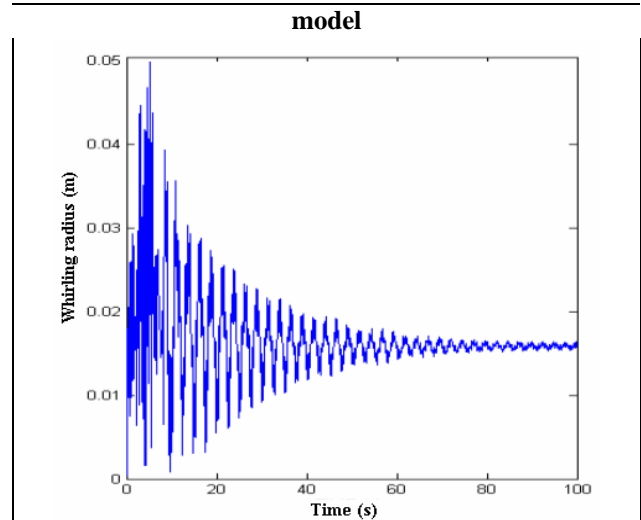


**Fig 11. Deflection at $\Omega = 8$ rad/s for fully coupled model**

Next the predictions of contact forces between wall and collar in critical angular velocity are investigated. Distribution and amplitude of contact forces predicted by both models are shown in Fig. 12 and 13. The fully coupled model predicts lower number of impacts and smaller impact force levels compared to the axial-lateral model predictions. The highest level of impact force is predicted as *1412 KN* using the axial-lateral model while the same value is predicted as *544 KN* by the fully coupled model. Also the number of impacts during a period of 100 sec in the results of axial-lateral model is 20169 while the other model predicts this value as 13903.

This is due to the fact that during impacts the applied torque on the collar reduces the collar angular velocity and the system rotates away from critical speed.

In the axial-lateral model this phenomenon is not included and therefore the impact forces and their sequence of occurrence are higher.
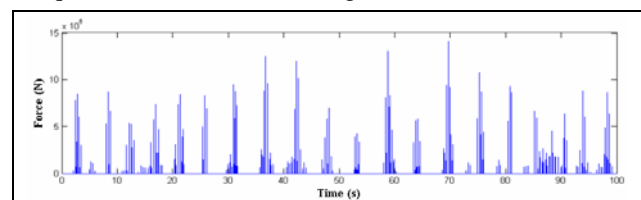


**Fig 12. Amplitude of contact force for $\Omega = 5.725$ rad/s (axial-lateral)**

The parametric resonance in drill string is reported in number of references ([8], [15], [16]). The followings investigates the parametric resonance in the system which happens when the frequency of applied forces are twice of the lateral natural frequency.
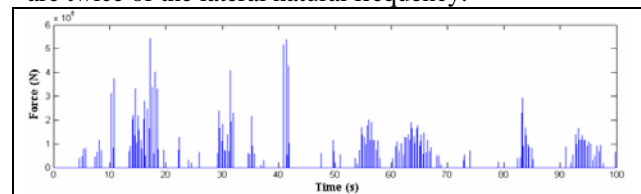


**Fig 13. Amplitude of contact force for $\Omega = 5.725$ rad/s (fully coupled)**

The loading frequency, $n\Omega$, is set as twice of the lateral natural frequency of drill string which is 5.725 rad/s. For a three cone bit (n=3), the critical angular velocity in parametric resonance is 3.817 *rad/s*.

Assuming zero eccentricity to eliminate the excitation due to unbalances the predicted responses of fully coupled model and the axial-lateral model are shown in figures 14 and 15. Both models show increase of amplitudes due to parametric resonance at 3.817rad/sec, but the fully coupled model predicts lower number of impacts due to the change in the rotational speeds.
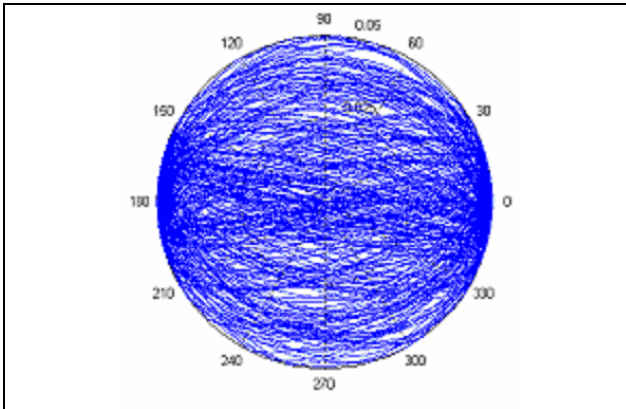


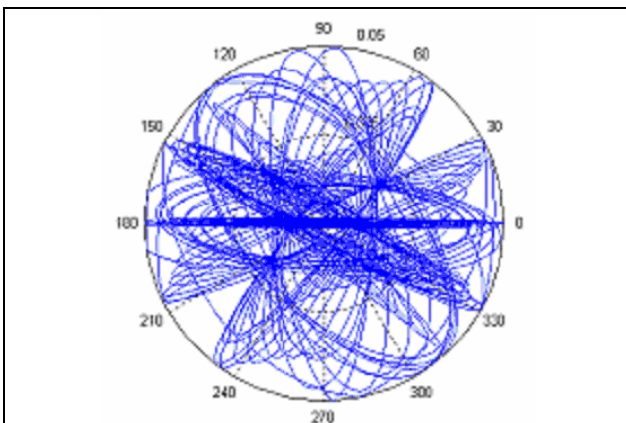**Fig 14. Radial deflection for** $\Omega = 3.817$ **rad/s and**
**$e_0$=0.0 (axial-lateral)**



**Fig 15. Radial deflection for** $\Omega = 3.817$ **rad/s and**
**$e_0$=0.0 (fully coupled)**

## 4. Conclusion

A fully coupled model for axial, lateral, and torsional vibrations of drill strings is presented and its predictions are compared with the conventional axial-lateral model results. A considerable difference between the results of the two models is observed. The fully coupled model predicts lower number of impacts and smaller impact force levels compared to the axial-lateral model predictions at the critical speeds. These differences can be explained considering the fact that during impacts the applied torque on the collar reduces the collar angular velocity and the system rotates away from critical speed. In the axial-lateral model this phenomenon is not included and therefore the impact forces and their sequence of occurrence are higher.

## References

[1] Finnie, I., & Bailey, J.J*., "An experimental study of drill string vibration"* American Society of Mechanical Engineers, Journal of Engineering for Industry, May 1960, PP. 129-135.

[2] Yigit, A.S., & Christoforou, A.P., *"Coupled torsional and bending vibrations of drill string s subject to impact with friction",* Journal of Sound and Vibration 215, 1998, PP. 167–181.

[3] Vandiver, J.K., Nichoison, J.W., & Rong-Juin Shyu *"Case studies of the bending vibration and whirling motion of drill collars"*, SPE, Drilling Engineering, 1990, PP. 282-290.

[4] Jansen, J.D., "*Non-linear rotor dynamic as applied to oil well drill string vibrations*", Journal of Sound and Vibration, Vol. 147, 1991, PP. 115-135.

[5] Jansen, J.D., Vanden, L., Steen & Erik Zachariasen, "*Active damping of torsional drill string vibrations with a hydraulic top drive*", SPE Drilling & Completion, December 1995, PP. 250-254.

[6] Abbassian, F., & Dunayevsky, V.A., *"Application of stability approach to torsional and lateral bit dynamic*", SPE Drilling & Completion, 1998, PP. 99-107.

[7] Yigit, A. S., & Christofourou, A.P., "*Coupled axial and transverse vibration of oil well drill string",* Journal of Sound and Vibration, Vol. 195, 1996, PP. 617-627.

[8] Christoforou, A.P., & Yigit, A.S., "*Dynamic modeling of rotating drill strings with borehole interactions",* Journal of Sound and Vibration, 206(2), 1997, PP. 243-260.

[9] Yigit, A.S., & Christoforou, A.P., *"Coupled torsional and bending vibration of drill strings subject to impact with friction"*, Journal of Sound and Vibration, Vol. 215(1), 1998, PP. 167-181,.

[10] Khulief, Y.A., & Al-Naser, H., **"***Finite element dynamic analysis of drill strings",* Finite Elements in Analysis and Design, Volume 41, Issue 13, July 2005, PP. 1270-1288.

[11] Khulief, Y.A., Al-Sulaiman, F.A., & Bashmal, S., **"***Vibration analysis of drill strings with self-excited stick–slip oscillations*", Journal of Sound and Vibration, Volume 299, Issue 3, 23 January 2007, PP. 540-558.

[12] Choi, S.H., Pierre, C., & Ulsoy, A.G., *"Consistent modeling of rotating timoshenko shaft subject to axial loads*", ASME Journal of Vibration and Acoustics, Vol. 114, April 1992, PP. 249-259.

[13] Goldsmith, W., Impact. LONDON: Edward Arnold, 1960.

[14] Al_Hiaddabi, S.A., Samanta, B., & Seibi, A., *"Non-Linear control of torsional and bending vibration of oilwell drill string"*, Journal of Sound and Vibration, Vol. 265, 2003, PP. 401-415,.

[15] Elsayed, M.A., Dareing, D.W., & Vonderheide, M.A., *"Effect of torsion on stability, dynamic forces and vibration characteristics in drill strings"*, ASME, Journal of Energy Resources Technology, Vol. 119, March 1997, PP. 11-19.

[16] Zainudio, C.A., Tlusty, J.L., & Dareing, D.W., *"Self-Excited vibration in drill string"*, SPE Paper 16661, 62$^{nd}$ Annual Conference, Dallas, TX, 1987, PP. 117-123.

## Appendix A

In order to develop the governing equations we substitute equations (16-17) into equations (12-14) to obtain the deformed shapes of the system. Next by forming the energy terms, equations of motion are obtained using Lagrange's equations, equation (11), In deriving the equations of motion only one mode is considered in the assumed responses, i.e. the one specified in equations (16) and (17). Choosing the generalized coordinate $q_i$ in equation (11) as $\alpha$ leads to:

$$
\left( \rho_c A_c \int_0^{l_1} \varphi dz + \rho_p A_p \int_{l_1}^{l} \varphi dz \right) \ddot{\alpha} + \left( E_c A_c \int_0^{l_1} \varphi_z^2 dz + E_p A_p \int_{l_1}^{l} \varphi_z^2 dz \right) \alpha
$$

$$
+ \frac{1}{2} \left( \beta^2 + \gamma^2 E_c A_c \int_0^{l_1} \varphi \zeta_z^2 dz \right) + \rho_c A_c \int_0^{l_1} \frac{\partial}{\partial t}\left(P_f \sin(\dot{\lambda}t)\right) \varphi dz +
$$

$$
\rho_p A_p \int_{l_1}^{l} \frac{\partial}{\partial t}\left(P_f \sin(\dot{\lambda}t)\right) \varphi dz + \int_0^{l} \left(P_0 + P_f \sin(\dot{\lambda}t)\right) \varphi_z dz =
$$

$$
\frac{l_1}{\rho_c A_c} \int_0^{l_1} \left(P_0 + P_f \sin(\dot{\lambda}t)\right) dz + \frac{1}{\rho_p A_p} \int_{l_1}^{l} \left(P_0 + P_f \sin(\dot{\lambda}t)\right) z dz +
$$

$$
\frac{l_1}{\rho_c A_c} \int_0^{l_1} \left(P_0 + P_f \sin(\dot{\lambda}t)\right) \varphi dz +
$$

$$
\frac{1}{\rho_p A_p} \int_{l_1}^{l} \left(P_0 + P_f \sin(\dot{\lambda}t)\right) z \varphi dz
$$

(22)

Second governing equation is obtained by choosing $q_i$ in equation (11) as $\beta$ :

$$
\int_0^l \left(\rho_c A_c \zeta^2 + \rho_c I_c \zeta_z^2\right) dz \ddot{\beta} + \left( \int_0^l \left(E_c I_c \zeta_{zz}^2 + \zeta_z^2\left(P_0 + P_f \sin(\dot{\lambda}t)\right)\right) dz \right) \beta +
$$

$$
\alpha\beta \int_0^l E_c A_c \zeta_z^2 \varphi_z dz - e_0 \dot{\lambda}^2 \sin(\dot{\lambda}t) \int_0^l \rho_c A_c \zeta dz
$$

$$
= \frac{F_N \left( \int_0^l \zeta_{zz} \zeta \dot{\beta} dz - sign\left( \frac{\zeta(z_c)\dot{\gamma}\beta^2 - \zeta(z_c)\gamma\dot{\gamma}\beta + R(\gamma^2 + \beta^2)}{\gamma^2 + \beta^2} \right) \mu\zeta(c)\gamma \right) \zeta(z_c)}{\sqrt{\left(\zeta(z_c)\gamma\right)^2 + \left(\zeta(z_c)\beta\right)^2}} -
$$

$$
\rho_f C_D R \int_0^l \left(\zeta\dot{\beta}\right)\sqrt{\left(\zeta\dot{\gamma}\right)^2 + \left(\zeta\dot{\beta}\right)^2} dz
$$

(23)

By employing equation (11) while $\gamma$ is the generalized coordinate one obtains the following equation:

$$
\left( \int_0^l \left(\rho_c A_c \zeta^2 + \rho_c I_c \zeta_z^2\right) dz \right) \ddot{\gamma} + \alpha\gamma \int_0^l E_c A_c \zeta_z^2 \varphi_z dz - e_0 \dot{\lambda}^2 \cos(\dot{\lambda}t)\int_0^l \rho_c A_c \zeta dz =
$$

$$
\frac{F_N \left( \zeta(z_c)\beta - sign\left( \frac{\zeta(z_c)\dot{\beta}\gamma^2 - \zeta(z_c)\gamma\dot{\gamma}\beta + R(\gamma^2 + \beta^2)}{\gamma^2 + \beta^2} \right) \mu\zeta(c)\gamma \right) \zeta(z_c)}{\sqrt{\left(\zeta(z_c)\beta\right)^2 + \left(\zeta(z_c)\gamma\right)^2}} -
$$

$$
\rho_f C_D R \int_0^l \left(\zeta^2\dot{\gamma}\right)\sqrt{\left(\zeta\dot{\gamma}\right)^2 + \left(\zeta\dot{\beta}\right)^2} dz
$$

(24)

Substituting equations (20) and (21) into equations (18) and (19) one obtains two following equations which are coupled with equations (22-24) and together form the set of equations governing the dynamic behavior of drill string :

$$
J_T \ddot{\phi} - K_{dp}(\lambda - \phi) = K_{up}(\Omega t - \phi) + C_{up}(\Omega - \dot{\phi})
$$

$$
+ 2\rho_c I_c \dot{\lambda}\dot{\beta}\int_0^l \zeta_{zz} \zeta dz
$$

(25)

$$
J_C \ddot{\lambda} + K_{dp}(\lambda - \phi) = W\left(f_0 - f_t e^{-\gamma\dot{\lambda}^*}\right) -
$$

$$
sign\left( \frac{\zeta(z_c)\dot{\beta}\gamma^2 - \zeta(z_c)\gamma\dot{\gamma}\beta + R\dot{\lambda}(\gamma^2 + \beta^2)}{\gamma^2 + \beta^2} \right)
$$

(26)

$$
\mu K_h (r - D_c)^{\frac{3}{2}} Heaviside \quad (r - D_c) R
$$